https://doi.org/10.3311/PPch.16612

Periodica Polytechnica Chemical Engineering, 65(3), pp. 343–349, 2021

Preparation and Characterization of SnO_2/AC as a Novel High Surface Area Nanocatalyst

Abdul Rahman Y. Wahoud[1*], Salim F. Bamsaoud[1], Mohammed A. Al-Haiqi[1]

[1] Chemistry Department, College of Science, Hadhramout University, P. O. B. 50511, Mukalla, Yemen
[*] Corresponding author, e-mail: awahoud8@gmail.com

Received: 06 June 2020, Accepted: 29 July 2020, Published online: 10 May 2021

Abstract

A new solid nanoparticle sorbent (SnO_2/AC) could serve as high surface area and inexpensive nanocatalyst was prepared. Many properties were characterized by SEM and UV spectroscopy. High surface area, large micro pore volume and total pore volume were found to be 571 $m^2\ g^{-1}$, 0.4785 $cm^3\ g^{-1}$ and 0.7267 $cm^3\ g^{-1}$ respectively even with very high loaded ratio (60 %) of tin dioxide to Activated Carbon (SnO_2/AC). Taguchi factorial design method was used to get the maximum MB dye adsorption on the surface of SnO_2/AC nanoparticle sorbent. Contact time (60 min), initial dye concentration (5 mM) and solution temperature (293 K) were found to be the best conditions for the more effective absorption process.

Keywords

nanocatalyst, Taguchi method, tin dioxide, Activated Carbon (AC)

1 Introduction

The most extensive work has been performed on the metals and their oxides supported on active carbon instead of SiO_2–Al_2O_3 [1–5]. They are considered to be as most promising catalysts because they are friendly environment and more active and selective, especially nanoparticles catalysts which have high surface area and large micro pore volume [6–8]. Various kinds of precursors have been modified with different materials and methods to produce high surface Activated Carbon (AC) such as peanut hulls [9], coconut husk [10], rice husk [11], bamboo [12], fruit stone [13] and papaya leaves [14]. Among of these agricultural wastes, Date Stones (DS) considered as the best candidate because it is cheap and abundantly available [15]. Moreover it has high surface area and it is easy to treated and activated [16, 17]. Taguchi statistical method was utilized in order to find out the ideal parameters for effective and maximum adsorption capacity of Methylene Blue (MB) dye with low cost of experiments and less time consuming [18, 19]. In this study we have prepared and characterized SnO_2/AC nanocatalyst and find out the ideal conditions for MB adsorption process by using statistical method. In addition to study and evaluate the adsorption performance of SnO_2/AC for the removal of MB from aqueous solutions to avoid environmental pollution.

2 Materials and methods

2.1 Materials

$SnCl_2 \cdot 2H_2O$, CH_3COOH, H_2SO_4, KOH, Acetone, Ethanol and Methylene Blue (MB) dye and all chemicals reagents in analytical grad were used from Uni-Chem.

Fig. 1 shows the MB dye structure (molecular formula $C_{16}H_{18}N_3SCl$, $3H_2O$, λ_{max} of 665 nm, Mw = 373.9 g mol^{-1}). It is recognized usefulness in characterizing adsorptive material and used as a model to remove colored contaminants from aqueous solutions.

2.2 Date Stone activation

Yemeni Date Stones (DS) washed several times with distillated water, dried, crushed and sieved with average particle size of 250 µm. Powder were soaked in 30 % KOH at room temperature with 1:20 weight ratio (DS: KOH) for 24 hour,

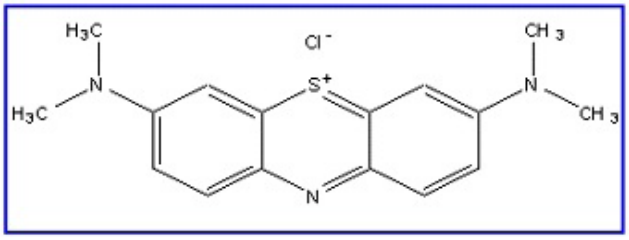

Fig. 1 Methylene Blue (MB) structure

Cite this article as: Wahoud, A. R. Y., Bamsaoud, S. F., Al-Haiqi, M. A. "Preparation and Characterization of SnO_2/AC as a Novel High Surface Area Nanocatalyst", Periodica Polytechnica Chemical Engineering, 65(3), pp. 343–349, 2021. https://doi.org/10.3311/PPch.16612

the solution was shake from time to another. Then potassium hydroxide solution was decanted and impregnated sample was put crucible with lid and carbonized by heated up to 648 K in muffle furnace for 2 hour. Then the sample was cooled and washed with of 0.01 M H_2SO_4 until the filtrate neutralization. After that, the Activated Carbon filtrated and dried at 378 K for 3 hours [17]. Table 1 shows the properties of raw Date Stone and Activated Carbon.

2.3 Preparation of SnO_2/AC nanocatalyst

SnO_2/AC nanocatalyst was prepared by precipitation of Sn(II) ions at Activated Carbon (AC), which we obtained from the Date Stones (DS), in aqueous solution. First, 2 g stannous chloride dissolved in 8 cm^3 of distilled water. Then 4 ml of glacial acetic acid was added into $SnCl_2$ solution and stirred for 1 h at 343 K. Then the solution was put in the oven at 673 K for 1.5 h to decompose all $SnCl_2$ and converted Sn II to SnO_2 nanoparticles [20]. After that a certain amounts of Activated Carbon and SnO_2 nanoparticles added to 25 cm^3 of distilled water and stirred continuously and heated until most of water evaporated. Then the sample was entered the oven for 2 h at 403 K. The SnO_2/AC nanocatalyst powder kept labeled in sealed glass flask for used in following experiments. The simple explanation of the mechanism of formation and growth of SnO_2 in the presence of Activated Carbon can be described by the following [20, 21]:

$$SnCl_2 \xrightarrow{\text{Aqueous solution}} Sn^{+2} + 2Cl^-$$

$$Sn^{+2} + CH_3COOH \xrightarrow{\text{Aqueous solution}} (CH_3COO)_2\,Sn + 2H^+$$

$$(CH_3COO)_2\,Sn \xrightarrow{\text{Oxidation 400 °C}} SnO_2 + CO_2 + CO$$

$$SnO_2 + AC \xrightarrow{\text{Aqueous solution}} SnO_2\,(AC)_{(aq)}$$

$$SnO_2\,(AC)_{(aq)} \xrightarrow{\text{Heat Treatment}} SnO_2\,(AC)_{(s)}\,.$$

2.4 Surface area and pore structure calculation

The surface area, micro pore volume (V_m) and total pore volume (V_t) of the samples were estimated by the following models [22]:

Table 1 Properties of DS and AC

Properties	DS	AC
Ash %	1.4	0.6
Moisture %	8	1.3
Bulk density (g cm^{-3})	0.76	0.2
Surface area (m^2 g^{-1})	563	750
Micropore volume (cm^3 g^{-1})	0.1545	0.9965
Total pore volume (cm^3 g^{-1})	0.4031	1.0055

$$S\left(\text{cm}^2\ \text{g}^{-1}\right) = 2.28\times10^{2} - 1.01\times10^{-1}\,\text{MBN} + 3.00\times10^{-1}\,\text{IN} + 1.05\times10^{-4}\,\text{MBN}^2 + 2.00\times10^{-4}\,\text{IN}^2 + 9.38\times10^{-4}\,\text{MBN}\times\text{IN} \quad (1)$$

$$V_m\left(\text{cm}^3\ \text{g}^{-1}\right) = 5.60\times10^{-2} - 1.00\times10^{-3}\,\text{MBN} + 1.55\times10^{-4}\,\text{IN} + 7.00\times10^{-6}\,\text{MBN}^2 + 1.00\times10^{-7}\,\text{IN}^2 - 1.18\times10^{-7}\,\text{MBN}\times\text{IN} \quad (2)$$

$$V_t\left(\text{cm}^3\ \text{g}^{-1}\right) = 1.37\times10^{-1} + 1.9\times10^{-3}\,\text{MBN} + 1\times10^{-4}\,\text{IN}, \quad (3)$$

where (IN) is Iodine Number and (MBN) is Methylene Blue Number.

2.5 Taguchi statistical method

The orthogonal array are used to conduct a set of experiments [18, 19], and *S*/*N* ratio are employed to study the performance characteristics of MB adsorption onto the prepared SnO_2/AC nanocatalyst. Four factors with three levels were designed in as shown in Table 2. A standard L_{27} array was used to determine the ideal conditions for maximum MB dye adsorption. The experimental results were shown in Table 3. The larger (*S*/*N*) ratio was selected to be the better. The *S*/*N* ratio is defined as [18]:

$$\frac{S}{N} = 10\log\frac{\left(1/Y_1^2 + 1/Y_2^2 + \ldots + 1/Y_n^2\right)}{n}, \quad (4)$$

where *n* the number of replicates and *y* is the experimental value.

2.6 Determination of Adsorption Capacity

To determine of adsorption capacity, 50 cm^3 of varying concentrations of MB dye were contacted with 0.5 g of every adsorbent placed in 250 cm^3 conical flask. The conical flask were tightly covered. The sample was putted

Table 2 Levels and factors

Factor	Level 1	Level 2	Level 3
Contact time (min)	15	30	60
Initial conc. (mM)	1	2.5	5
SnO_2/AC ratio (%)	10	20	40
Temperature (K)	293	313	333

Table 3 The surface area and pore volume at different SnO_2/AC ratio

SnO_2/AC %	S (cm^2 g^{-1})	V_m (cm^3 g^{-1})	V_t (cm^3 g^{-1})
0	690	0.9965	1.0055
10	670	0.8627	0.8853
20	632	0.6342	0.8116
40	604	0.5469	0.7655
60	571	0.5185	0.7267

at room temperature (298 ± 2 K) on a magnetic stirrer with a thermostat to control the temperature, to reach equilibrium. All experiments were performed at 555 rpm.

Then the samples were filtered and analyzed by a ultraviolet Spectrophotometer (Jasco V-730) at λ_{max} 665 nm. The uptake of MB dye adsorbed q_t on SnO_2/AC surface was calculated as following:

$$q_t = \frac{(C_0 - C_t)}{W} \times V, \tag{5}$$

where C_0 and C_t (mg dm^{-3}) are the initial and equilibrium of MB dye concentrations respectively, V (dm^3) is the solution volume and W (g) is the weight of Date Stone.

3 Results and discussion

3.1 SnO_2/AC characterizations

Fig. 2 shows the ultraviolet spectrum for SnO_2 solution, it has an absorption peak at 295 nm which corresponds to band gap energy of ~4.2 eV, which indicates nanoparticle size comparable to that of the bulk Bohr exciton radius found to be ~2.7 nm [20, 23]. The XRD data for SnO_2 nanopartical (Fig. 3) shows that all the peaks are related to SnO_2 tetragonal phase which were confirmed with the standard JCPDS data (No. 72-1147). No other peaks were present related to any phase of SnO_2. The peaks 26.6, 33.7 and 51.7° were considered to calculate the average crystallite size using Scherer formula and the crystallite size was found to be 8 nm. In agreement with XRD data the TEM and SEM for SnO_2 nanopartical (Figs. 4, 5) shows that the size was about 8 nm. The Scanning Electron Microscope (SEM) of the SnO_2/AC surface (Fig. 6) clearly indicates that the nanostructures of SnO_2/AC which we obtained

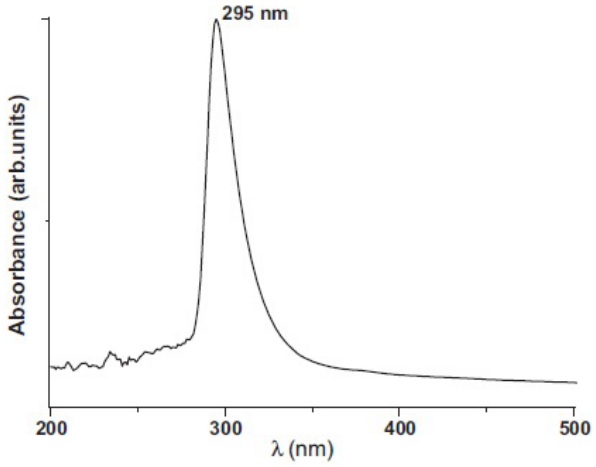

Fig. 2 UV–Vis spectra of the transparent SnO_2 solution

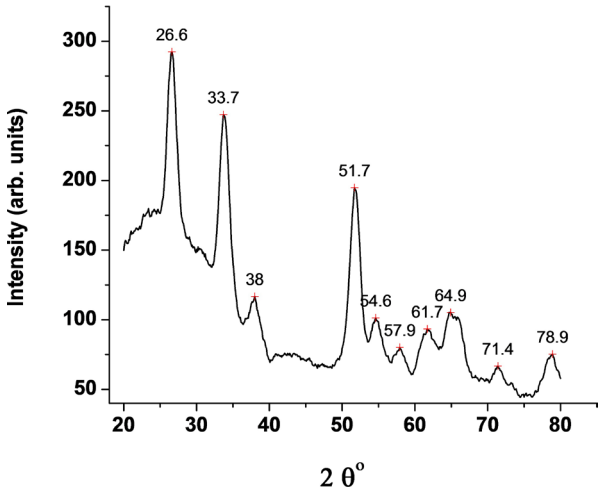

Fig. 3 XRD of the SnO_2 nanopartical

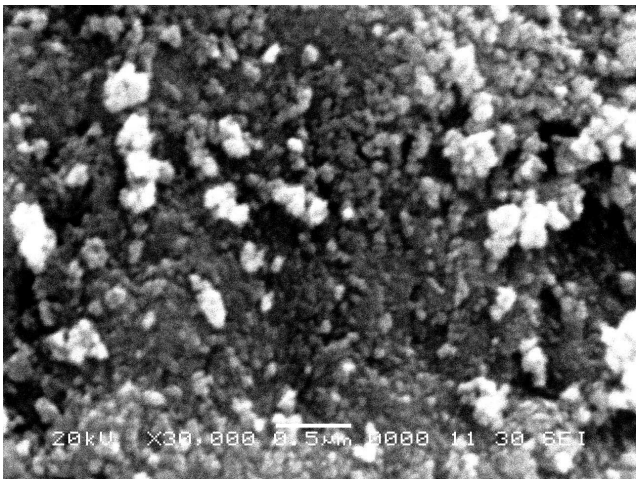

Fig. 4 SEM of the SnO_2 nanoparticle surface

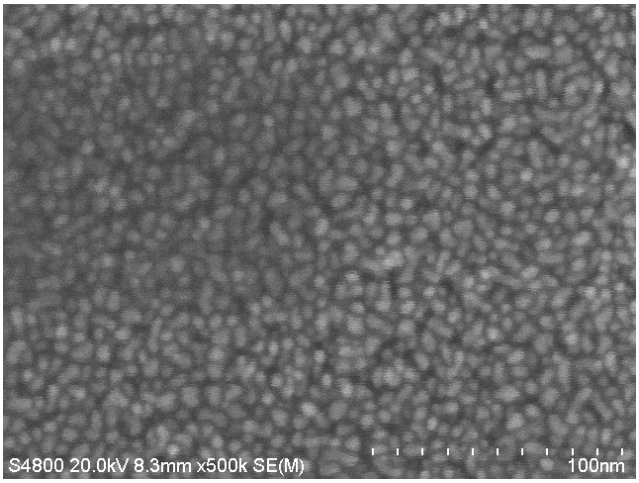

Fig. 5 TEM of the SnO_2 nanoparticle surface

and shows a good scattering of SnO_2 inside the pores of Activated Carbon and no SnO_2 crystallites were found out of the pores.

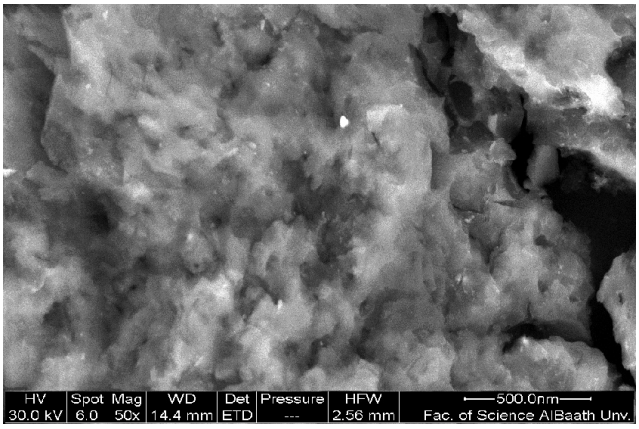

Fig. 6 SEM of the SnO_2/AC nanocatalyst

3.2 Mechanism of control of SnO_2/AC nanocatalyst formation

The effect of reaction conditions in the synthesis of SnO_2/AC on the surface area and pore volume of nanocatalyst (Fig. 6) was studied by loading different mass present ratios of tin dioxide to Activated Carbon SnO_2/AC (0, 10, 20, 40, 60, 100 wt%) according to the experimental procedures. The result was put in the Table 3. It clear that, although the surface area and pore volume decrease by increasing the SnO_2/AC ratio, but they haven't affected so much and the SnO_2/AC 60 % nanocatalyst still have a high surface area 571 $cm^2\ g^{-1}$ with large micropores volume 0.4785 $cm^3\ g^{-1}$ and large total pores volume 0.7267 $cm^3\ g^{-1}$, this indicates that the nanoparticles of tin dioxide don't agglomerate and don't blog the pores. They don't crystalline outside of the pores.

3.3 Effects of parameters on the adsorption process

To study the effects of parameters on the MB dye adsorption onto SnO_2/AC nanocatalyst, Taguchi factorial design method was used. The results for each experiment were put in Table 4. The results show that the uptake of MB varied from 32.49 mg g^{-1} to 237.96 mg g^{-1}, and *S*/*N* ratios

Table 4 L_{27} orthogonal arrays

Expt. No.	Contact time (min)	Initial conc. (mM)	SnO_2/AC ratio (%)	Temperature (K)	Uptake (mg g^{-1})	*S*/*N* ratio
1	15	1	10	293	40.23	32.09
2	15	1	10	313	36.52	31.25
3	15	1	10	333	32.49	30.23
4	15	2.5	20	293	73.47	37.32
5	15	2.5	20	313	70.77	36.99
6	15	2.5	20	333	67.83	36.62
7	15	5	40	293	96.63	39.70
8	15	5	40	313	94.11	39.47
9	15	5	40	333	92.54	39.32
10	30	1	20	293	57.92	35.25
11	30	1	20	313	55.24	34.84
12	30	1	20	333	53.22	34.52
13	30	2.5	40	293	141.91	43.04
14	30	2.5	40	313	137.77	42.78
15	30	2.5	40	333	135.43	42.63
16	30	5	10	293	205.11	46.23
17	30	5	10	313	203.12	46.15
18	30	5	10	333	201.34	46.07
19	60	1	40	293	60.07	35.57
20	60	1	40	313	58.65	35.36
21	60	1	40	333	56.34	35.01
22	60	2.5	10	293	155.76	43.84
23	60	2.5	10	313	153.73	43.73
24	60	2.5	10	333	151.88	43.63
25	60	5	20	293	237.96	47.53
26	60	5	20	313	233.71	47.37
27	60	5	20	333	230.18	47.24

Table 5 *S/N* value and rank of each factor

Level	Contact time (min)	Initial conc. (mM)	SnO_2/AC ratio (%)	*T* (K)
1	35.89	33.79	40.36	40.06
2	41.28	41.17	39.74	39.77
3	42.14	44.34	39.21	39.47
Delta	6.25	10.55	1.15	0.59
Rank	2	1	3	4

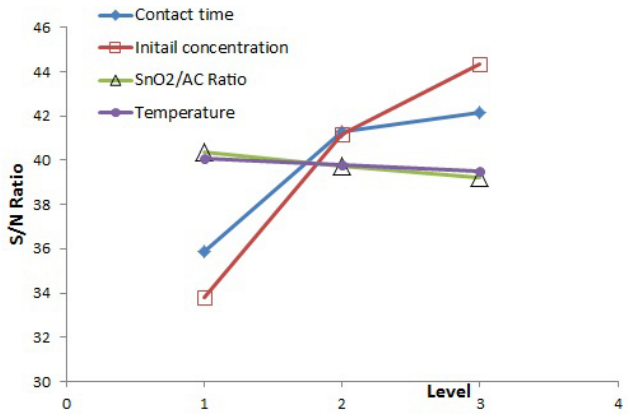

Fig. 7 *S/N* ratios with levels of different factors

from 30.23 to 47.53. From Table 5 and Fig. 7, level 3 was found to be the best for each contact time and initial dye concentration factors, and level 1 was found to be the best for SnO_2/AC ratio and temperature factors. On the other hand, the order of importance of factors for the MB adsorption into SnO_2/AC nanocatalyst is initial dye concentration, contact time, SnO_2/AC ratio and temperature respectively, and the best uptake amount of MB dye is 237.96 mg g^{-1} with ideal conditions.

3.4 Effect of contact time

From Fig. 7, it is clear that the contact time is an important parameter for the dye uptake. The *S/N* ratio increases by increasing the contact time from 15 min to 60 min and the highest MB uptake reached at contact time 60 min at third level. This may be due to of active sites and functional groups available on the surface of SnO_2/AC nanocatalyst at the beginning of the adsorption process.

3.5 Effect of initial MB dye concentration

To study the effect of MB initial concentration on the adsorption, different concentration of MB solutions (1, 2.5, 5 mM) were prepared. The results was put in Table 5 and represented in Fig. 7. The results shows that the *S/N* ratio increases by increasing the MB initial concentration and the highest MB uptake achieved at the third level of MB initial concentration (5 mmol). This may be due to a lot of pores and active sites on the surface of SnO_2/AC adsorbent are available.

3.6 Effect of temperature

The effect of temperature on the adsorption was investigated in three levels of temperature (293, 313, 333 K). The results which represented in Fig. 7 which shows that the *S/N* ratio decreases by increasing temperature.

In the other hands, the MB dye uptake decreases by increasing temperature and was achieved the lowest value at level 3 of temperature.

This may be due to the weak attraction between MB and adsorbent surface shown in Fig. 8, and the increasing of temperature leads to the MB molecules to escape from the surface [24, 25].

3.7 Effect of SnO_2/AC ratio

The obtained results show that the *S/N* ratio decreases by increasing of SnO_2/AC ratio. On the other words, the smallest *S/N* ratios value and the highest MB uptake occurred at ratio of 10 % SnO_2/AC. It means that the SnO_2/AC ratio is the least important variable influencing the dye uptake and the efficiency of MB dye adsorption decreases neglectably with the increasing SnO_2/AC ratio. This may be due to the nanoparticles size SnO_2 is less than the size of micropores and loading more SnO_2 nanoparticles doesn't bloke the micropores, so the surface area of SnO_2/AC still large enough to affect the efficiency of MB adsorption very much.

4 Conclusion

An Activated Carbon modified tin oxide nanoparticle (SnO_2/AC) as a novel inexpensive nanocatalyst was synthesized and characterized. The new SnO_2/AC nanocatalyst balances many of the properties such as high surface area and effective adsorption power that researches have looking for, and could pave the way toward safe and environmentally friendlier alternatives for economical chemical industry. We find that the best conditions for the

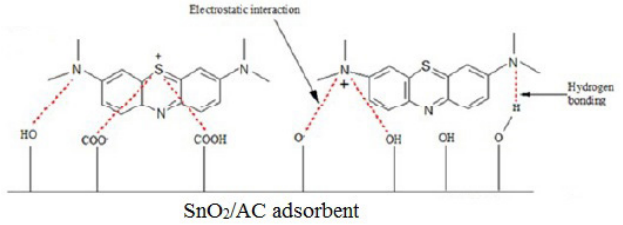

Fig. 8 Mechanism of MB dye adsorption into SnO_2/AC

adsorption of MB dye onto SnO_2/AC from solution were 10 % for SnO_2/AC ratio, 60 min for contact time, 5 mM for initial MB concentration and 298 K for temperature.

Acknowledgement
We gratefully acknowledge Hadhramout University for assist and support of the project presented in this article.

References

[1] Otsuka, K., Ogihara, K., Takenaka, S. "Decomposition of methane over Ni catalysts supported on carbon fibers formed from different hydrocarbons", Carbon, 41(2), pp. 223–233, 2003. https://doi.org/10.1016/S0008-6223(02)00308-1

[2] Ermakova, M. A., Ermakov, D. Y., Kuvshinov, G. G. "Effective catalysts for direct cracking of methan to produce hydrogen and filamentous carbon: Part I. Nickel catalysts", Applied Catalysis A: General, 201(1), pp. 61–70, 2000. https://doi.org/10.1016/S0926-860X(00)00433-6

[3] Liu, J., Zhao, Z., Xu, C., Duan, A., Zhu, L., Wang, X. "Diesel soot oxidation over supported vanadium oxide and K-promoted vanadium oxide catalysts", Applied Catalysis B: Environmental, 61(1–2), pp. 36–46, 2005. https://doi.org/10.1016/j.apcatb.2005.04.006

[4] Chimentão, R. J., Herrera, J. E., Kwak, J. H., Medina, F., Wang, Y., Peden, C. H. F. "Oxidation of ethanol to acetaldehyde over Na-promoted vanadium oxide catalysts", Applied Catalysis A: General, 332(2), pp. 263–272, 2007. https://doi.org/10.1016/j.apcata.2007.08.024

[5] Nguyen, L. D., Loridant, S., Launay, H., Pigamo, A., Dubois, J. L., Millet, J. M. M. "Study of new catalysts based on vanadium oxide supported on mesoporous silica for the partial oxidation of methane to formaldehyde: Catalytic properties and reaction mechanism", Journal of Catalysis, 237(1), pp. 38–48, 2006. https://doi.org/10.1016/j.jcat.2005.10.016

[6] Tanaka, A., Yoon, S.-H., Mochida, I. "Formation of fine Fe–Ni particles for the non-supported catalytic synthesis of uniform carbon nanofibers", Carbon, 42(7), pp. 1291–1298, 2004. https://doi.org/10.1016/j.carbon.2004.01.029

[7] Huwe, H., Fröba, M. "Synthesis and characterization of transition metal and metal oxide nanoparticles inside mesoporous carbon CMK-3", Carbon, 45(2), pp. 304–314, 2007. https://doi.org/10.1016/j.carbon.2006.09.021

[8] Huwe, H., Fröba, M. "Iron (III) oxide nanoparticles within the pore system of mesoporous carbon CMK-1: intra-pore synthesis and characterization", Microporous and Mesoporous Materials, 60(1–3), pp. 151–158, 2003. https://doi.org/10.1016/S1387-1811(03)00336-6

[9] Ding, Z., Hu, X., Zimmerman, A. R., Gao B. "Sorption and cosorption of lead (II) and methylene blue on chemically modified biomass", Bioresource Technology, 167, pp. 569–573, 2014. https://doi.org/10.1016/j.biortech.2014.06.043

[10] Tan, I. A. W., Ahmad, A. L., Hameed, B. H. "Adsorption of basic dye on high-surface-area activated carbon prepared from coconut husk: Equilibrium, kinetic and thermodynamic studies", Journal of Hazardous Materials, 154(1–3), pp. 337–346, 2008. https://doi.org/10.1016/j.jhazmat.2007.10.031

[11] Safa, Y., Bhatti, H. N. "Kinetic and thermodynamic modeling for the removal of Direct Red-31 and Direct Orange-26 dyes from aqueous solutions by rice husk", Desalination, 272, pp. 313–322, 2011. https://doi.org/10.1016/j.desal.2011.01.040

[12] Hameed, B. H., Din, A. T. M., Ahmad, A. L. "Adsorption of methylene blue onto bamboo-based activated carbon: Kinetics and equilibrium studies", Journal of Hazardous Materials, 141(3), pp. 819–825, 2007. https://doi.org/10.1016/j.jhazmat.2006.07.049

[13] Lussier, M. G., Shull, J. C., Miller, D. J. "Activated Carbon from Cherry Stones", Carbon, 32(8), pp. 1493–1498, 1994. https://doi.org/10.1016/0008-6223(94)90144-9

[14] Krishni, R. R., Foo, K. Y., Hameed, B. H. "Adsorption of methylene blue onto papaya leaves: comparison of linear and nonlinear isotherm analysis", Desalination and Water Treatment, 52(34–36), pp. 6712–6719, 2014. https://doi.org/10.1080/19443994.2013.827818

[15] Adinata, D., Wan Daud, W. M. A., Aroua, M. K. "Preparation and characterization of activated carbon from palm shell by chemical activation with K_2CO_3", Bioresource Technology, 98(1), pp. 145–149, 2007. https://doi.org/10.1016/j.biortech.2005.11.006

[16] Belala, Z., Jeguirim, M., Belhachemi, M., Addoun, F., Trouvé, G. "Biosorption of basic dye from aqueous solutions by Date Stones and Palm-Trees Waste: Kinetics, equilibrium, and thermodynamic studies", Desalination, 271(1–3), pp. 80–87, 2011. https://doi.org/10.1016/j.desal.2010.12.009

[17] Hameed, B. H., Salman, J. M., Ahmad, A. L. "Adsorption isotherm and kinetic modeling of 2,4-D pesticide on activated carbon derived from date stones", Journal of Hazardous Materials, 163(1), pp. 121–126, 2009. https://doi.org/10.1016/j.jhazmat.2008.06.069

[18] Rahmani, M., Kaykhaii, M., Sasani, M. "Application of Taguchi L16 design method for comparative study of ability of 3A zeolite in removal of Rhodamine B and Malachite green from environmental water samples", Spectrochimica Acta Part A: Molecular and Biomolecular Spectroscopy, 188, pp. 164–169, 2018. https://doi.org/10.1016/j.saa.2017.06.070

[19] Ghasemi, M., Mashhadi, S., Azimi-Amin, J. "Fe_3O_4/AC nanocomposite as a novel nano adsorbent for effective removal of cationic dye: Process optimization based on Taguchi design method, kinetics, equilibrium and thermodynamics", Journal of Water Environmental Nanotechnology, 3(4), pp. 321–336, 2018. https://doi.org/10.22090/jwent.2018.04.005

[20] Bamsaoud, S. F., Rane, S. B., Karekar, R. N., Aiyer, R. C. "SnO_2 film with bimodal distribution of nano-particles for low concentration hydrogen sensor: Effect of firing temperature on sensing properties", Materials Chemistry and Physics, 133(2–3), pp. 681–687, 2012. https://doi.org/10.1016/j.matchemphys.2012.01.052

[21] Agashe, C., Aiyer, R. C., Garaje, A. "High-Yield Synthesis of Nanocrystalline Tin Dioxide by Thermal Decomposition for Use in Gas Sensors", International Journal of Applied Ceramic Technology, 5(1), pp. 181–187, 2008. https://doi.org/10.1111/j.1744-7402.2008.02196.x

[22] Nunes, V. A., Guerreiro, M. C. "Estimation of Surface Area and Pore Volume of Activated Carbons by Methylene Blue and Iodine Numbers", Química Nova, 34(3), pp. 472–476, 2011. https://doi.org/10.1590/S0100-40422011000300020

[23] Bamsaoud, S. A., Rane, S. B., Karekar, R. N., Aiyer, R. C. "Nano particulate SnO_2 based resistive films as a hydrogen and acetone vapour sensor", Sensors and Actuators B: Chemical, 153(2), pp. 382–391, 2011. https://doi.org/10.1016/j.snb.2010.11.003

[24] Lee, E. J. H., Ribeiro, C., Giraldi, T. R., Longo, E., Leite, E. R. "Photoluminescence in quantum-confined SnO_2 nanocrystals: Evidence of free exciton decay", Applied Physics Letter, 84(10), pp. 1745–1747, 2004. https://doi.org/10.1063/j.snb.1.1655693

[25] Manna, S., Roy, D., Saha, P., Gopakumar, D., Thomas, S. "Rapid methylene blue adsorption using modified lignocellulosic materials", Process Safety and Environmental Protection, 107, pp. 346–356, 2017. https://doi.org/10.1016/j.psep.2017.03.008